PROCEEDINGS OF SCIENCE

Monitoring of high-intensity muon beams

M. Bonesini*
Sezione INFN Milano Bicocca, Dipartimento di Fisica G. Occhialini,
Universitá di Milano Bicocca, Milano, Italy
E-mail: bonesini@mib.infn.it

High intensity low energy muon beams are crucial tools for fundamental physics and applied research. The good steering of the incoming beam on the experimental target or the sample under study is essential. For this task, beam monitors, to provide informations on beam profile and intensity, have been realized with many different techniques and some of them will be reviewed in this paper.

The 19th International Workshop on Neutrinos from Accelerators-NUFACT2017
25-30 September, 2017
Uppsala University, Uppsala, Sweden

*Speaker.

PoS(NuFact2017)159

1. Introduction

Low energy muon beams of high-intensity are required in many scientific areas from particle physics to fundamental atomic physics, condensed matter physics and beyond. Results in this field (high intensity frontier) are often limited by the available muon statistics. Up to now beams with an integrated rate of 10^{15} muons/year are available, but new experiments may require much higher rates. As an example, charged lepton flavour violation (CLFV) experiments as $\nu \to e\gamma$ [1] and $\mu \to eee$ [2] require beam intensities up to $\sim 10^{18}$ muons/year. Even more stringent requirements are set for muon colliders [3], where beam intensities up to 10^{21} muons/year are needed.

Muon beams are usually produced via charged pion decays in proton target collisions. Surface muons [4] are produced from π at rest at the target surface and have a defined momentum of 29.7 MeV/c, as the pion decay is a two-body process. The resulting μ momentum spectrum outside the production target extends to lower momentum due to muons produced below the target surface. The polarization of a surface muon beam is $\sim 100\%$ and only positive muons are available, as negative muons are captured inside the target by the atomic nuclei. Ultra slow muons, with momenta in the eV-keV range, may be obtained by further reducing the energy of a surface muon beam by using a moderator.

Decay muons, both positive and negative, are instead produced by $\pi \to \mu$ decay in flight. Pions are collected over a certain solid angle by quadrupoles and then decay in a section consisting mainly of a long superconducting solenoid. By a suitable momentum selection of both π and μ, only backward $\pi \to \mu\nu$ decays are considered. In this case, the momentum difference between the muons and the pion beam residual contamination is greater, giving a cleaner beam. For such a beam, higher momenta (typically 40-120 MeV/c) are available and the polarity may be selected by changing the currents in the bending magnets.

Muon beams may be further classified according to the time structure of the used accelerator: continuos (DC) or pulsed. In pulsed beams, the secondary beam muons have a structure that reflects the one of the main proton accelerator. As an example, at RIKEN-RAL [5] two pulses of 70 ns (FWHM) width are separated by 320 ns, with a repetition cycle of 50 Hz. Typically DC beams are used for coincidence experiments (e.g. $\mu \to e\gamma$), while pulsed beams are used for non coincidence experiments (e.g. $\mu \to e$ conversion).

Some characteristics of conventional surface (decay) muon beamlines are resumed in table 1 (2), where some examples are reported. As can be seen, the rate of surface μ^+ is larger than the rate of decay μ^+, while the rate for decay μ^- is even lower.

Future developments, aiming at rates in the range $10^{11} - 10^{12}\mu$/s, are foreseen both for pulsed beamlines, as PRISM [6] and DC beamlines as HiMB at PSI [7].

As an example, the layout of RIKEN-RAL muon facility at ISIS is shown in figure 1. Either decay or surface muons may be produced, to be sent to four experimental areas (Port 1, ... Port 4). The ISIS primary proton beam at 800 MeV/c, with a 50 Hz repetition rate, impinges from the left on a secondary carbon target producing a high-intensity pulsed muon beam, that reflects the primary beam structure. For decay muons at ~ 60 MeV/c, the intensity is around $6 \times 10^4 \mu^-/s$, with an energy spread $\sim 10\%$ and an angular divergence ~ 60 mrad.

Muon beamlines are usually designed and optimized using particle transport codes as TRANSPORT [8] or TURTLE [9]. An example is reported in reference [10] for the μE4 beam at PSI.

PoS(NuFact2017)159

Table 1: Examples of surface muon beamlines in use

laboratory/beam	power/energy	surface μ^+ rate (Hz)
RAL-ISIS EC RIKEN-RAL	800 MeV,160 kW, pulsed	 4×10^5 1.5×10^6
PSI LEMS πE5	550 MeV, 1.3 MW, DC	 4×10^8 1.6×10^8
KEK DAI OMEGA	500 MeV, 2.5kW, pulsed	 4×10^5
JPARC MUSE D-line	3 GeV,1 MW, pulsed currently 210kW	 3×10^7
TRIUMF M20	500 MeV, 75kW, DC	 2×10^6
Dubna Phasotron Ch I-III	660 MeV, 1.65 kW, pulsed	 3×10^4
RCNP Osaka MUSIC	400 MeV, 400 W, pulsed currently 4 W	 10^8

Table 2: Examples of decay muon beamlines in use

laboratory/beam	power/energy	μ^+ (μ^-) rate (Hz)
RAL-ISIS RIKEN-RAL	800 MeV,160 kW, pulsed 20-120 MeV/c	 3×10^5 (6×10^4) at 60 MeV/c
JPARC MUSE D-line	3 GeV, 1 MW, pulsed currently 210 kW 5-120 MeV/c	 few 10^6 at 60 MeV/c

2. Monitoring of high intensity muon beams

A tertiary muon beam has a very low current rate as compared to the primary proton beam: pA as compared to μA-mA. Thus "non-destructive" techniques based on electromagnetic pickups or wire profile monitors may not be used, as signals would be too small. Only "destructive techniques" based on energy deposition measurement in scintillator counters or similar detectors may be used. Thus the beam monitors must be removed from beamline, during normal data taking. An exception may be with decay muon beams of higher energy.

Monitoring of a muon beamline may involve both rate measurements (beam intensity) and beam profile measurements, to help the optimization of the beam steering onto the target.

Muon beam monitors may be realized with very different devices, such as ion chambers or proportional wire chambers, as at the Muon Campus at FNAL [11], gated image Intensifiers, as at JPARC MUSE [12] or more conventional instrumentation based on thin scintillators or scintillating fibers. Each type of detectors has its own advantages or disadvantages. In the following we will

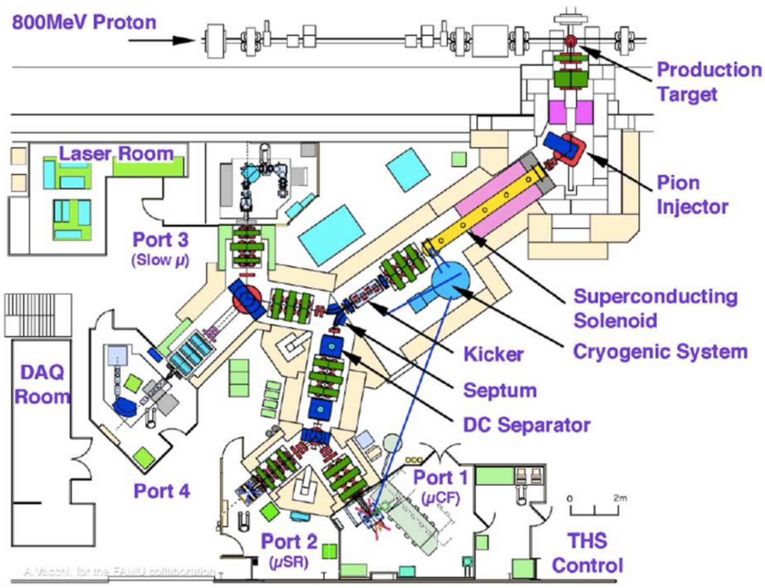

Figure 1: Layout of the RIKEN-RAL facility at RAL.The four experimental areas (Port1-Port4) are shown. Both surface muons and decay muons may be produced.

discuss in depth only muon monitors based on scintillators.

3. Muon beam monitors

Some examples of muon beam monitors using as active devices thin scintillators or scintillating fibers are resumed in table 3. The readout devices may be photomultipliers (PMTs), multianode photomultipliers (MPMTs), avalanche photodiodes (APDs) or silicon photomultipliers (SiPM). The front-end electronics is usually based on a charge integrating ADC (QADC) or a FADC that provide informations on the recorded waveforms, such as total charge, peak pulse height, timing...

Table 3: Examples of muon beam monitors based on scintillators or scintillating fibers.

ref	beamline	active device	detector structure	readout	electronics
[13]	PSI μE4	POLIFI 1 mm round fibers	10(X)× 10(Y) fibers with 10 mm spacing	APD	VME multiscaler
[14]	JPARC MUSE	0.5 mm thick NE102 scint.	15(X) × 15(Y) 4mm strips, 10 mm spacing	MPMT	CAMAC QADC
[15]	JPARC MUSE	100 μm fibers	one layer (100 mm)	SiPM	Easiroc chip [16]
[17]	RIKEN surface μ	0.5 mm thick NE102 scint.	4(X) × 4(Y) 4mm strips, 10 mm spacing	PMT	CAMAC QADC
[18]	RIKEN decay μ	BCF12 fibers	32(X) × 32(Y) 3mm square fibers	Advansid SiPM	custom TPS + VME QADC
[19]	RIKEN decay μ	BCF12 fibers	32(X) × 32(Y) 1 (3) mm square fibers	Hama/Adv. SiPM	VME FADC

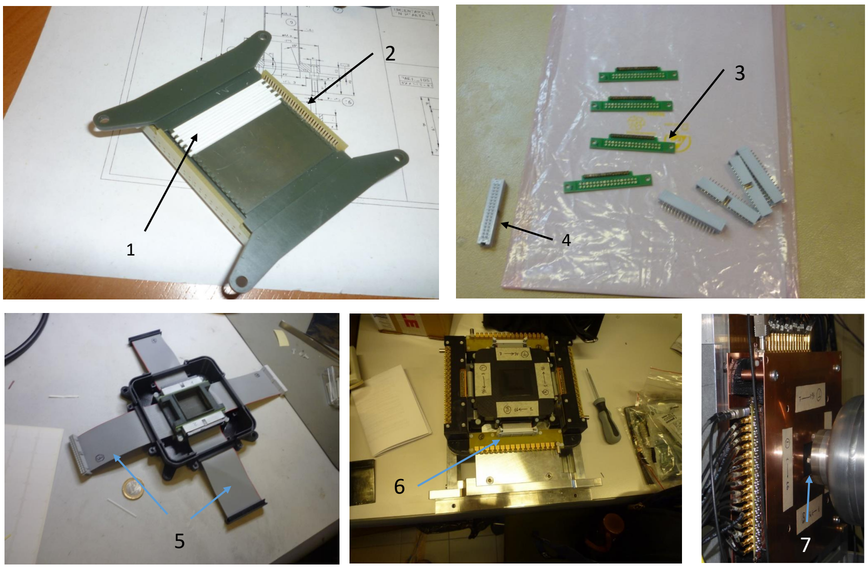

Figure 2: Construction details of the 1 mm pitch hodoscope of the FAMU experiment at RIKEN-RAL. Top left panel: fiber holder with some 1 mm square fibers (1) and the PCB (2) on which SiPM are soldered; top right panel: details of some PCBs (3) and the 20-way connectors (4). Bottom left panel: fiber holders with 40-way flat cables mounted (5); bottom middle panel: detector with interface boards mounted (6); detector with shielding copper plate in front of the beam collimator (7) at RIKEN-RAL.

Some construction details of the 1 mmm pitch FAMU hodoscope of reference [19] are shown in figure 2. Its design is based on single clad Bicron BCF12 square scintillating fibers with EMA to avoid light cross-talk. They have a peak emission $\sim$ 435 nm, a 4.4% trapping efficiency and a 2.7 m bulk attenuation length. The light yield is $\sim$ 8000 photons/MeV. The readout is based on Advansid RGB SiPM with 40 μm cells and CAEN V1742 FADC.

A two dimensional image (X/Y) of the beam spot is shown for the same hodoscope in figure 3, together with the plot of the recorded total charge (Q_{tot}) that may be used for beam intensity monitoring.

The FAMU 3 mm pitch hodoscope has a similar structure based on BCF12 3×3 mm^2 square fibers read by SiPM. At first Advansid RGB SiPM with 40 μm cells were used. Later they were replaced by Hamamatsu S12752 SiPM with 25 μm cells, to increase the dynamic range, at the expense of an increased operating voltage. The readout for the 3 mm pitch hodoscope was first realized with a custom electronics based on the INFN TPS project [20] and VME CAEN V792 QADCs and then replaced by a standard VME electronics based on a CAEN V1742 digitizer.

In addition to what reported in table 3, some interesting *R&D* efforts were pursued. As an example, the MEG experiment at PSI has tried to develop an active target (ATAR) that could act both as a target for the experiment and a beam monitor. Based on a single layer of 250 μm Bicron scintillating fibers, read by SiPM, it used as readout the DRS4 FADC chip developed at PSI [21]. Test results are reported in reference [22].

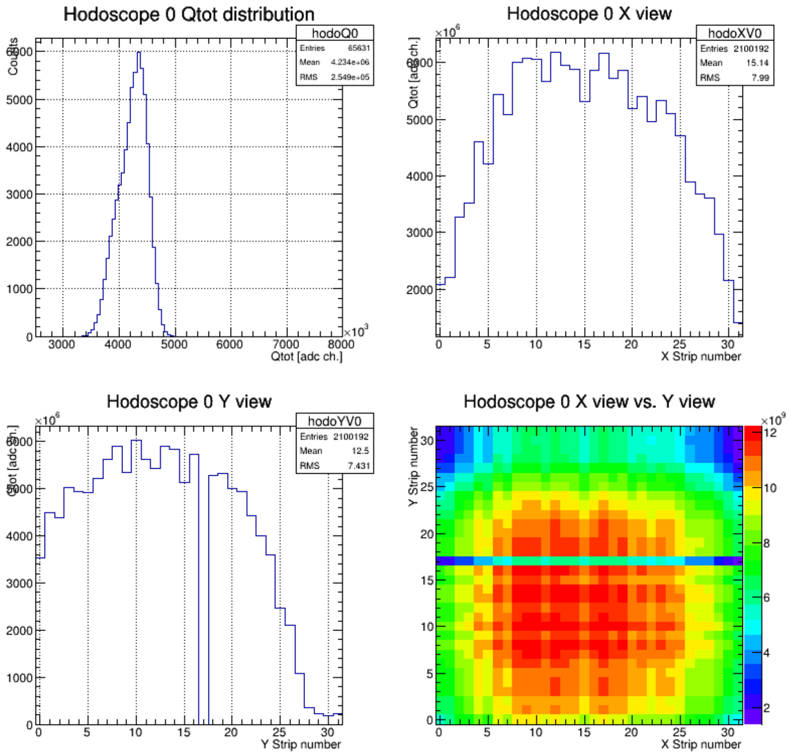

Figure 3: Beam spot of the muon beamline at RIKEN-RAL, as recorded at the entrance of the FAMU experiment. One channel of the hodoscope was not connected to the FADC in the considered run.

4. Conclusions

Many beam monitors of different design have been developed for existing low-energy muon beams, to improve the beam steering. In this paper we focus on the more conventional scintillator option, that has evolved from the use of thin scintillator slabs read by PMTs to the use of scintillating fibers coupled to SiPMs.

Acknowledgements

I would like to thank all the colleagues of the FAMU collaboration at RAL, in particular Dr. E. Mocchiutti, Prof. A. Vacchi, Dr. M. Rossella and Dr. L. Tortora and Dr. K. Ishida from RIKEN-RAL, for help and advice.

References

[1] J. Adams *et al.*, [MEG Coll.], *New Constraint on the Existence of the* $\mu^+ \to e^+\gamma$ *Decay*, *Phys. ReV. Lett.*. **110** 201801 (2013).

[2] A.Blondel *et al.*, *Research Proposal for an Experiment in search of the decay* $\mu \to eee$, *arXiv:1301.6113*

[3] M. Bonesini, Perspectives for Muon Colliders and Neutrino Factories, Frascati Phys. Ser. **61** (2016) 11;

M. Bogomilov *et al.*, *N*eutrino Factory, *P*hys. RevST Accel. Beams **17** (2014) no 12, 121002;
M.A.Alsharoa *et al.*, *R*ecent progress in neutrino factory and muon collider research within the Muon collaboration, *P*hys. RevST Accel. Beams **6** (2003) 081001.

[4] A.E. Pifer *et al.*, *A* high stopping density μ^+ beam, *N*ucl. Instr. Meth. **135** (1976) 39

[5] T.Matsuzaki *et al.*, *T*he RIKEN-RAL pulsed Muon Facility, *N*ucl. Instr. Meth. **A465** (2001) 465

[6] R.J.Barlow, *T*he PRISM/Prime Project, *N*ucl. Phys. B Proc. Suppl. **218**(2011) 44

[7] A. Knecht, *T*he high-intensity muon beamline (HiMB) project at PSI, these proceedings

[8] PSI Graphic TRANSPORT Framework, by U. Rohrer based on CERN-SLAC-FERMILAB version by K.L. Brown

[9] PSI Graphic TURTLE Framework, by U. Rohrer based on CERN-SLAC-FERMILAB version by K.L. Brown

[10] T.Prokscha *et al.*, *The new μE4 beam at PSI*, *N*ucl. Instr. Meth. **A595** (2008) 317.

[11] D.Stratakis *et al. I*nstrumentation and its interaction with the secondary beam for the Fermilab Muon Campus, *M*OPAB141 (2017)

[12] T.U.Ito *et al*, *O*nline Monitoring of Negative Muon Beam Profiles at J-PARC MUSE using a Gated Image intensifier, *J*PS Conf. Proc. **8** (201‘5) 036012.

[13] A. Stoykov *et al.*, *A* scintillating fiber detector for muon bram profile measurements in high magnetic fields, *N*ucl. Instr. Meth. **A550** (2005) 2012.

[14] P. Strasser *et al.*, *J*-PARC Decay Muon Channel Construction Status, *J*our. Phys. Conf. series **225** (2010) 012050.

[15] S. Kanda *et al.*, *D*evelopment of online muon beam profile monitor for the MuSEUM experiment, RIKEN Accel. Progr. Rep . 48 (2015)

[16] S.Callier *et al. E*ASIROC, an EASY & Versatile Readout Device for SiPM *P*hysics Procedia **37** (2012) 1569.

[17] P. Strasser *et al.*, *A* beam profile monitor for RIKEN-RAL pulsed muon beam, *R*IKEN Accel. Prog. Rep. **36** (2003) 202

[18] R.Carbone *et al.*, *T*he fiber-SIPMT beam monitor of the R484 experiment at RIKEN-RAL muon fascility, *J*INST (2014) **10** C03007.

[19] M. Bonesini *et al.*, *T*he construction of the fiber-SiPM beam monitor system of the R484 and R582 experiment at the RIKEN-RAL muon facility, *JINST* **12** C03035 (2017).

[20] P.Branchini *et al.*, *A*n FPGA based general purpose DAQ module for the KLOE-2 experiment, *I*EEE Trans. Nucl. Sci. **58** (2011) 1544;
R.Plesack *et al. T*he FIRST experiment at GSI, *N*ucl. Instr. Meth. **A678** (2012) 130.

[21] S. Ritt *et al.*, *A*pplication of the DRS chip for fast waveform digitizing, *N*ucl. Instr. Meth. **A623** (2010) 486.

[22] A. Papa *et al.*, *F*easibility study of an active target for the MEG experiment, Nucl. Phys. B Proc Suppl. **248** (2014) 121;
A.Papa *et al.*, *A* multi-purpose detector with Silicon photomultiplier readout of scintillating fibers, *N*ucl. Instr. Meth. **A787** (2015) 130.